Structure and Properties of Vacuum-Deposited Cadmium Thin Films

N. C. Halder

Department of Physics, University of South Florida, Tampa, Florida

Z. Naturforsch. **34a**, 176–187 (1979); received September 21, 1978

Thin films of Cd were prepared by vacuum deposition onto glass plates at temperature of 45 °C and pressure of about 10^{-6} torr. Several good quality films of various thicknesses (15,000 ~ 28,000 Å) were made. The films were characterized by strong preferred orientation along the 002 planes parallel to the surface of the substrate, which were found to be thickness dependent. In particular, the 002, 100 and 004 peaks were many times stronger than their corresponding diffraction peaks obtained from powder specimens. Both the real and imaginary parts of the Fourier coefficients were considered for line broadening analysis. The particle size (which is also called the average size of the coherently diffracting domains in a direction perpendicular to the diffracting planes), microstrain (which is usually called the mean strain in a given direction) and faulting were determined. A systematic study for all the diffraction peaks indicates an increase of average particle size $\overline{D}$ from 546 to 620 Å in the above thickness range with no apparent anisotropy for the 100, 002 and 004 directions. The microstrain, however, decreased as much as 50% in this thickness range and showed a considerable amount of anisotropy. The fault parameters α (deformation fault probability) and β (growth fault probability) decreased rather rapidly for all directions.

1. Introduction

This is the third paper in our series of publications on the x-ray diffraction study (XDS) of hexagonal close packed (hcp) metals. In our earlier papers [1, 2] (hereafter will be referred to as paper I and paper II), we have studied the x-ray line broadening phenomena in deformed hcp polycrystalline Cd, Mg and Zn powders. In the present paper we report a complementary study in evaporated thin films of Cd. The microstructure of powder samples of metals and alloys has been extensively studied [3–5], by x-ray diffraction method over the period of last two decades and many important advancements have been made in the theory and application by such studies. However, only a few corresponding studies [6–15] have been reported in the thin films of metals and alloys. The main reasons are that (i) the microcrystallites in thin films are not randomly deposited such as found in powders, (ii) films should be very uniform, sufficiently thick and good quality for XDS measurement, and (iii) the corrections due to geometrical effect and preferred orientation are not easy to perform experimentally. On the other hand, the phenomena of thin films have become a very important field of research, because of their many interesting features and variety of applications. The purpose of this investigation is to understand the structural defects and properties in thin films of hcp metals. Although Cd has rather high vapor pressure, this metal was selected because we have already studied its structural properties in the powder form, but no such study exists in the thin films of this metal except some preliminary studies by us [13].

0340-4811 / 79 / 0200-0176 $ 01.00/0

2. Experimental

2.1. Preparation of Thin Films

Thin films of Cd were prepared with various thicknesses by evaporation onto microscopic glass substrates using a Kinney vacuum system. The apparatus consisted of a resistance heated Mo boat and a metal plate positioned above it. The plate served two purposes: first a circular hole in the plate directly above the boat acted as a mask for the substrate placed on top of the plate, and secondly the plate shielded most of the heat radiations coming from the heating resistance. The sides of the bell jar were also shielded with sheets of Al foil. Glass microscope slides were used for the substrates. To clean each slide, it was placed in dilute solution of sodium hydroxide, rinsed with distilled water, placed in dilute solution of nitric acid, rinsed with distilled water, and finally rinsed with ethyl alcohol. The clean slide was then clamped lightly in position on top of the hole in the mask.

Metal shots of purity 99.999% were obtained from Apache Chemicals. For each film, a few small pieces were placed in the Mo boat, with the clean substrate and the mask directly above the boat. For all of the films prepared, the distance between the boat and the substrate was 4 cm. The bell jar was

pumped down to a pressure of about 10^{-6} torr, and then current through the boat was slowly turned on. The film thicknesses were controlled by controlling the current through the heating resistance and time of deposition. A calibration curve was first obtained with current and time for thickness monitoring before the experimental films were made. The film thicknesses were measured outside the vacuum chamber by the gravimetric method. The films were identified in the increasing order of thicknesses. This is illustrated in Table 1. The film temperature was not monitored, but kept constant throughout the experiment for all the films. A number of heat shields were used to stop the stray heat radiations.

Films	Thickness
A	14,700 Å
B	22,000 Å
C	25,300 Å
D	27,700 Å

Table 1. Thicknesses of the Cd films prepared at about a pressure of 10^{-6} torr onto microscopic glass substrates at 45 °C.

2.2. Recording of X-ray Diffraction Pattern

The x-ray diffraction patterns of the thin films were recorded [3, 4] on a vertical Philips diffractometer with the flat sample focusing condition. The Ni-filtered CuKα radiation was used. The x-ray beam was collimated through 1° divergence slit and passed through .006° receiving slit. Each diffraction peak was scanned at 1/8° per minute scanning speed and recorded at 30 inches per hour paper chart speed. The intensity scale, the baseline and the time constant were adjusted each time, depending on the intensity and broadening of the peak. Because of the importance of the peak tails, care was taken to collect the background level over sufficiently large angular spread on either side of the peak maximum. Seven diffraction peaks 002, 100, 101, 102, 103, 004 and 104 were recorded.

In recording the diffraction pattern, it was noticed that certain peaks in the thin films were much stronger than the corresponding peaks in the powder sample. In particular, the 002, 100 and 004 peaks were many times stronger; however, the 101, 102 and 103 peaks were somewhat less stronger. On the other hand, the 110 and 112 peaks were much weaker in films than in powder. The Miller indices were assigned from the computed Bragg angles (shown in Table 2) using the theoretical

Table 2. Integral breadth of the measured peaks. The unit used is 10^3 radians.

Peaks	*A*	*B*	*C*	*D*
002	1.24	1.23	1.12	1.31
100	1.38	1.08	1.06	1.26
101	1.32	1.11	1.11	1.36
102	1.49	1.13	1.18	1.27
103	1.15	1.22	1.08	1.22
004	1.13	1.12	1.11	1.18
104	1.34	1.59	1.23	1.44

lattice parameters for Cd, $a = 2.9787$ and $c = 5.6170$ A. In order to analyze the diffraction peaks, data points at equal intervals of 0.025° in two theta were tabulated for computation.

The experimental profiles were first subjected to various correction procedures before analyzing them. The first one is the application of Lorentz polarization (LP) factor [16, 17] due to non-polarized x-ray beam and the second one is the removal of α_2 doublet [18—21] of the Cu radiation.

About required separation of the CuKα_1 peak from CuKα_2 peak, a number of suggestions have been made [11, 19] in recent years illustrating some essential differences in the various computational procedures. In reality, however, the traditional Rachinger method [20, 21] is still applicable and could be used when some of the suggested changes in the paper of Gangulee [11], and Delhez and Mittemeijer [19] (DM) are included. In the Gangulee [11] method one can separate the α_1 peak from α_2 by direct use of the Fourier coefficients as in the Stokes procedure. But in the DM procedure, an angular dependent doublet separation function is introduced within a particular peak. For example, the intensities of the two peaks are related to the observed peak by

$$h_\alpha(2\theta) = h_{\alpha_1}(2\theta) + h_{\alpha_2}(2\theta) \tag{2.1}$$

and $$h_{\alpha_1}(2\theta - \delta) = C_1 h_{\alpha_2}(2\theta)$$

$$\text{where } C_1 = 2\,, \tag{2.2}$$

in which δ is the angular separation between α_1 and α_2 peak maximum. In the original work of Rachinger δ was substituted to be a constant

$$\delta = 2\theta_1 - 2\theta_2 \tag{2.3}$$

which in the paper by DM was replaced by angular dependent functions, such as,

$$\delta_\lambda = 2 \arcsin\left(\frac{\lambda_2}{\lambda_1} \sin\theta_1\right) - 2\theta_1 \tag{2.4}$$

or

$$\delta_B = 2 \tan\theta \, \Delta\lambda / \langle\lambda\rangle \, . \tag{2.5}$$

The later improvement, which is theoretically more appropriate, certainly gives very little or no oscillations towards the high angle side of the diffraction peak under study. It is now well understood that these oscillations are not due to any termination or computational errors in the data analysis procedure rather due to the effect of constant δ function used earlier. In principle the Rachinger method is not wrong but angular dependent doublet separation function δ must be used [22, 23] to minimize errors. In many investigations, a crystal monochromator can be placed in the path of the primary beam to reduce the intensity peak ratio of the $K\alpha_2$ and $K\alpha_1$ to a significantly small value. In such experiments, the Rachinger or any other method of separation is totally unnecessary. Light and Wagner [5] used this procedure in their study of Ag films.

3. Computer Analysis of the Experimental Data

3.1. The Geometrical Correction for Thin Films

For powder samples, whenever structural deformations are investigated at room temperature or lower than room temperature, it has become almost a routine procedure to extract the geometrical profile by annealing a portion of the deformed sample to a very high temperature for sufficient length of time so that all the mechanical stress and strain are completely washed out within the experimental detection. Another method, although not very common, is to use the diffraction profile of a powder of another sample where previous studies indicated negligible or no x-ray line broadening due to mechanical deformation, for example quartz or calcite powder. If, however, the line profile to be investigated is quite broad, no such geometrical correction is necessary, since the percentage error to be introduced in such a case would be very small compared to other sources of errors usually encountered in XDS. This is especially applicable to amorphous solids, liquids and, perhaps, polymers.

The problem we are facing with regard to geometrical correction in the study of thin films is quite different and cannot be handled by the methods summarized above. First of all, preparation of a standard sample by annealing a thin film deposited on a glass substrate is out of the question, since it is not practically feasible. Furthermore, the diffraction lines from thin films have considerably less broadening, but a lot of preferred orientation. Therefore, application of another sample, such as quartz or calcite, was equally unwarranted. Under the circumstances, we shall proceed to solve this problem analytically by performing a detailed computer analysis of all the measured diffraction lines.

We shall write the normalized physical Fourier coefficients as complex quantities

$$F'(L) = A(L) + i\,B(L) = \frac{H_r' + i H_i'(L)}{G_r'(L) + i\,G_i'(L)} \tag{3.1}$$

where $H'(L)$ represents the Fourier coefficient of the measured profile and $G'(L)$ that of the geometrical profile. By simple algebra, we get

$$A(L) = \frac{H_r'(L)\,G_r'(L) + H_i'(L)\,G_i'(L)}{G_r'^2(L) + G_i'^2(L)} \tag{3.2}$$

and

$$B(L) = \frac{H_i'(L)\,G_r'(L) - H_r'(L)\,G_i'(L)}{G_r'^2(L) + G_i'^2(L)} \, . \tag{3.3}$$

In the Fourier analysis of the actual diffraction peaks one has to determine both cosine and sine coefficients. Because the imaginary part, i. e., sine part of the coefficients, were treated very small in the past, the coefficients $A(L)$ were approximated to

$$A(L) \cong H_r'(L)/G'(L) \, . \tag{3.4}$$

If, however, the imaginary parts are not small, then their effects would be propagated into the elastic strain and particle-size-faulting coefficients. Very recently de Keijser and Mittemeijer [22] have noted this effect and made some attempt to remove this inconsistency. We shall, however, discuss here both the real and imaginary parts of all the Fourier coefficients. From Warren-Averbach theory we have

$$\begin{aligned} F'(L) &= A(L) + i\,B(L) \\ &= A^{PF}(L)(A^D(L) + i\,B^D(L)) \end{aligned} \tag{3.5}$$

where the particle size faulting coefficients $A^{PF}(L)$ are real numbers that do not depend on the order of reflection. Quite contrary to this the strain

coefficients are complex. We then find that

$$A(L) = A^{PF}(L)\, A^{D}(L) \tag{3.6}$$

and

$$B(L) = A^{PF}(L)\, B^{D}(L)\,. \tag{3.7}$$

3.2. Real Part of the Fourier Coefficient

From the theory of Fourier analysis we can get, for small strain values,

$$\begin{aligned} A^{D}(L) &\cong 1 - 2\pi^2 L^2 e_L{}^2/d_{hkl}^2 \\ &\cong \exp[-2\pi^2 L^2 e_L{}^2/d_{hkl}^2] \end{aligned} \tag{3.8}$$

where

$$e_L = \langle \varepsilon_L{}^2 \rangle^{1/2} \tag{3.9}$$

is the root mean square strain.

The particle size-faulting coefficients are shown [16] to be

$$A^{PF}(L) = 1 - L/D_{eff} \tag{3.10}$$

where D_{eff} is the effective particle size that includes faulting. Then

$$\begin{aligned} \ln H_r'(L) &= \ln(1 - L/D_{eff}) \\ &\quad - (2\pi^2 L^2/d_{hkl}^2)\, e_L{}^2 + \ln G'(L) \end{aligned} \tag{3.11}$$

where $H'(L)$ is still complex, but $G'(L)$ is assumed to be real. This is due to the fact that there is little asymmetry due to structural deformation. We shall then consider that the geometrical profiles of these reflections are symmetrical functions. These will be represented by Gaussian functions for the sake of analytical computation. A logical choice, which we shall elaborate momentarily, would be to write it, similar to the strain coefficients,

$$G'(L) = \exp\left\{-\frac{2\pi^2 K}{d_{hkl}^2} L^2\right\} \tag{3.12}$$

where K is a geometrical parameter that does not depend on the sample at all. It is then possible to obtain the geometrical profile, by making inverse Fourier transform of Eq. (3.12),

$$g(x) = \frac{d_{hkl}}{\sqrt{2\pi K}} \exp\left(-\frac{d_{hkl}^2}{2K} x^2\right). \tag{3.13}$$

Thus, we find, in absence of any appropriate practical standard sample,

$$\ln H_r'(L) = \ln(1 - L/D_{eff}) - \frac{2\pi^2}{d_{hkl}^2}(e_L{}^2 + K) L^2\,. \tag{3.14}$$

If we were to include the effect of preferred orientation as well, it would still be possible to proceed in the above manner. The peak broadening with different hkl arises from various microcrystallite orientations in the film which are strong functions of certain crystallographic direction and could be identified with d_{hkl}. We then introduce another parameter S for preferred orientation and rewrite the above equation as

$$\begin{aligned} \ln H_r'(L) &= \ln(1 - L/D_{eff}) \\ &\quad - \frac{2\pi^2}{d_{hkl}^2}(e_L{}^2 + K + S) L^2\,. \end{aligned} \tag{3.15}$$

Thus a plot of $\ln H_r'(L)$ against $1/d_{hkl}^2$ should be a straight line for constant L when reflections representing the same crystallographic direction are used.

It should be recognized here that D_{eff} is equivalent to D for 002 and 004 reflections in hcp samples. The particle size effect in thin films, unlike powder samples, is single crystal-like. That is, the size of the coherently diffraction domain is sufficiently large enough so as to be considered as negligible in the above equation. Then, to a good approximation, one can write

$$\ln H_r'(L) \cong -\frac{2\pi^2}{d_{hkl}^2}(e_L{}^2 + K + S) L^2 \tag{3.16}$$

making $\ln H_r'(L)$ against L^2 plot go through the origin. Any deviation from the origin is a quantitative measure of the amount of particle size effect.

As it is seen clearly from Eqs. (3.15) and (3.16) the meaning of the slope is more complicated than that observed in powder samples. Nevertheless, it is possible to elaborate on the nature and various factors that contribute to the geometrical parameter K and the preferred orientation parameter S.

3.3. Imaginary Part of the Fourier Coefficient

The imaginary part of the strain coefficient is the average of sine functions

$$\begin{aligned} B^{D}(L) &= \langle \sin 2\pi L\, \varepsilon_L/d_{hkl} \rangle \\ &\cong 2\pi L \langle \varepsilon_L \rangle / d_{hkl} \\ &= 2\pi L\, \bar{e}_L/d_{hkl}\,, \end{aligned} \tag{3.17}$$

where $\bar{e}_L$ is the mean strain. Thus we can get

$$B(L) = (1 - L/D_{eff})(2\pi L\, \bar{e}_L/d_{hkl})\,. \tag{3.18}$$

When using the coefficients of the measured diffraction peaks directly, we obtain from Eqs.

(3.13), (3.12) and (3.18) (3.19)

$$\ln H_i'(L) = \ln(1 - L/D_{\text{eff}}) + \ln\left(\frac{2\pi L \bar{e}_L}{d_{hkl}}\right) - \frac{2\pi^2}{d_{hkl}^2}(K+S)L^2 .$$

This equation is strongly nonlinear in d that does not have any simple solution as is this case described by its real counterpart in Equation (3.15). Nevertheless, we still can extract a lot of information by taking advantage of a pair of reflections representing the same crystallographic direction. In the present case reflection 002 and 004 will be suitable. So for this pair of reflections

$$(\ln H_i'(L))_{002} = \ln(1 - L/D_{\text{eff}}) + (2\pi L \bar{e}_L/d_{002}) - 2\pi^2 L^2 (K+S)/d_{002}^2$$

and

$$(\ln H_i'(L))_{004} = \ln(1 - L/D_{\text{eff}}) + (2\pi L \bar{e}_L/d_{004}) - 2\pi^2 L^2 (K+S)/d_{004}^2 .$$

Recognizing that $d_{002} = 2d_{004}$, we find that

$$(4 \ln H_i'(L))_{004} - (\ln H_i'(L))_{002} = 3\ln(1 - L/D_{\text{eff}}) + 3\ln(2\pi L \bar{e}_L/d_{002}) - \ln 2. \quad (3.20)$$

By this process of elimination we have succeeded in removing the difficulty of nonlinearity appearing through the $1/d_{hkl}^2$ term. Since the first term of Eq. (3.20) is already known from the real counterpart as shown in Eq. (3.15) we can easily now determine $\bar{e}_L$ for any desired value of L.

3.4. Exact Nature of the Geometrical Parameter K

The geometrical broadening in the diffraction peak is due to one or more of the following causes [24, 25]: (i) projected source function, (ii) sample displacement function, (iii) axial divergence function, (iv) sample transparency function, (v) receiving slit function, (vi) sample misalignment function, and (vii) spectral width function. We denote these functions respectively by $g_1, g_2, g_3, g_4, g_5, g_6$ and g_7. The geometrical broadening is then expressed as convolution of all these,

$$g(x) = g_1 * g_2 * g_3 * g_4 * g_5 * g_6 * g_7 \quad (3.21)$$

where the asterisks mean successive convolution of the various g-functions. It is enormously difficult, perhaps impossible, to evaluate the convolution integral since there is no known exact way to measure or generate these functions. However, some attempts have been made [16] to represent these functions by appropriate analytical forms.

It has been shown [16] that the functions g_1, g_5, g_6 and g_7 are symmetric functions, whereas g_2, g_3 and g_4 asymmetric. The effect of these asymmetric functions is difficult to determine, but fortunately for us this effect maybe perfected to zero by performing experiments intelligently and carefully. As for example, a symmetrical profile obtained with diformation-free-standard quartz or calcite powder will be indicative of vanishingly small effect of the above asymmetric functions. After making several tests on the experimental set up over wide angular range, one can make the effect of the asymmetric functions completely disappear.

We are now left with the effect of the symmetric functions alone, which are inherent to every diffraction experiment and that must be removed analytically. We now make Fourier transform of the functions g_1, g_5, g_6 and g_7 to obtain the geometrical coefficient

$$G(L) = \left(\frac{\pi^2}{k_1 k_5 k_6 k_7}\right) \cdot \exp\left[-\pi^2 L^2\left(\frac{1}{k_1^2} + \frac{1}{k_5^2} + \frac{1}{k_6^2} + \frac{1}{k_7^2}\right)\right] \quad (3.22)$$

where k's are constants for the respective functions which may be estimated experimentally. Normalizing this coefficient as before, we find

$$G'(L) = \exp\left[-\pi^2 L^2\left(\frac{1}{k_1^2} + \frac{1}{k_5^2} + \frac{1}{k_6^2} + \frac{1}{k_7^2}\right)\right] \quad (3.23)$$

On comparison of this equation with Eq. (3.12), we obtain

$$K = \left(\frac{1}{k_1^2} + \frac{1}{k_5^2} + \frac{1}{k_6^2} + \frac{1}{k_7^2}\right)\frac{d_{hkl}^2}{2}. \quad (3.24)$$

Theoretically K is computable from the experimental conditions of the apparatus, sample geometry and value of the wavelength used. It has been recently pointed out by Delhez et al. [22, 23] that both the instrumental function g_i ($=g_1, g_5, g_6$) and the spectral function g_s ($=g_7$) always do contribute to the geometrical broadening in any given experiment; however, they weigh the geometrical broadening differently depending on the actual angular position of the diffraction peak.

They have demonstrated that g_s is more important than g_i in the small angular range, but it reverses itself in the high angular range.

4. Results and Discussions

4.1. Peak Heights, Peak Shapes and Peak Breadths

To record a diffraction peak for Fourier analysis, it is not necessary to measure [21] the intensity in absolute unit, but it is important to compare the peak intensities among themselves on the same scale. We have observed that 002 reflection was the strongest followed by 100 reflection. The reflections 101, 102 and 103 were relatively less strong. The reflection 104 was not detected in randomly prepared polycrystalline samples. The peak heights of all the reflections showed gradual enhancement when the thickness of the films was raised from 14,700 to 27,700 Å.

The peak shapes were affected very little with thickness. In general the peaks were not absolutely symmetrical. The high angle peaks were rather broad, but quite strong so as to be meaningfully included in the Fourier analysis. The integral breadth, which is defined as the area under the peak divided by the peak hieght, showed some definite decrease with thickness. The experimental points as tabulated in Table 2 show some scattering, which is due to the extrasensitivity of the very strong peaks, a characteristic of thin film samples. When these points are plotted this difficulty, however, does not appear, and a smooth set of data points are easily obtained.

4.2. Features of the Real and Imaginary Parts of Fourier Coefficients

The Fourier coefficients of 100, 002, and 004 reflections are shown in Figs. 1a—d. We have plotted both the real and imaginary parts of all coefficients to illustrate their respective behavior. In the past the effect of the imaginary part was considered trivial, and hence it was completely ignored for any kind of quantitative use. H_r' is always positive and attains a maximum value of 1 as $L \to 0$ for all reflections. On the other hand, H_i' is negative in most part and tends to zero value as $L \to 0$. In the thickness range considered, H_i' curves have the longest amplitude for 100 reflection. This means that 100 reflection must exhibit the highest microstrain due to structural disorder. The oscillations for 004 reflection seem to be more rapid than the others. They do not, however, become positive until about $L = 200$ Å. Each one of these H_i' curves has a number of very distinct features and one can identify them quite readily. The real parts of the coefficients are relatively featureless. Nevertheless, they become totally separable in the region of large L.

For the reflections with faulting we have plotted in Figs. 2a and 2b the total Fourier coefficient H'; separate plots of H_i' and H_r' are not necessary as they do not give any additional information. The general characteristics of 101, 102, 103 and 104 are very similar.

4.3. Particle Size amd Microstrain

It is well established [4] that for hcp structures the reflections satisfying $h - k = 3N$

$$(\mathrm{d}A^{\mathrm{PF}}/\mathrm{d}L)_{L=0} = -1/D \tag{4.1}$$

where N is an integer. These reflections are 002 and 004 in the present case. But due to the difficulty pointed out in Section III, we are forced to select an alternative approach. We return to Eq. (3.15) and take the first derivative to obtain

$$\frac{\partial H_r'(L)}{\partial L} = -\frac{4\pi^2 L}{d_{hkl}^2}(e_L^2 + K + S) \cdot (1 - L/D) \exp\left[-\frac{2\pi^2}{d_{hkl}^2}(e_L^2 + K + S) L^2\right] - \frac{1}{D}\exp\left[-\frac{2\pi^2}{d_{hkl}^2}(e_L^2 + K + S) L^2\right] \tag{4.2}$$

which in the limit $L \to 0$ reduces to

$$(\partial H_r'(L)/\partial L)_{L=0} = -1/D\,. \tag{4.3}$$

Proceeding in the same manner we find from Eq. (3.19), for the imaginary part of the coefficient,

$$\frac{\partial H_i'}{\partial L} = -\frac{4\pi^2 L}{d_{hkl}^2}(K + S)(1 - L/D)(2\pi \bar{e}_L/d_{hkl}) \cdot \exp\left[-\frac{2\pi^2}{d_{hkl}^2}(K + S)\right] + \frac{2\pi \bar{e}_L}{d_{hkl}}(1 - L/D) \cdot \exp\left[-\frac{2\pi^2}{d_{hkl}^2}(K + S)\right] - \frac{2\pi \bar{e}_L L}{d_{hkl} D} \cdot \exp\left[-\frac{2\pi^2}{d_{hkl}^2}(K + S)\right]. \tag{4.4}$$

This simply gives in the limit $L \to 0$

$$(\partial H_i'/\partial L)_{L=0} = 2\pi \bar{e}_L/d_{hkl}\,. \tag{4.5}$$

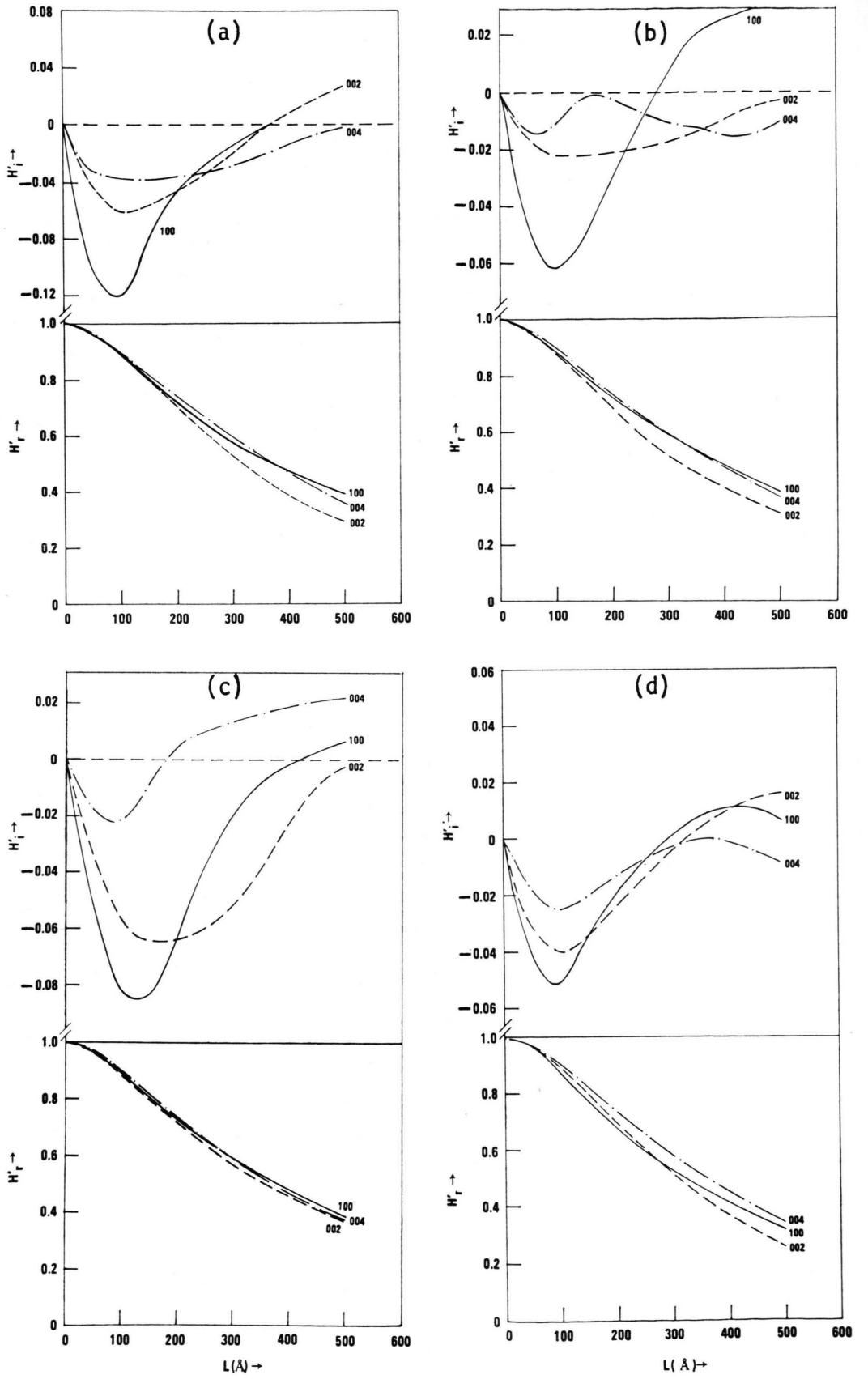

Fig. 1. The plots of real H_r' and imaginary H_i' parts of the Fourier coefficients of Cd thin films (a) Film A; (b) Film B; (c Film C; (d) Film D.

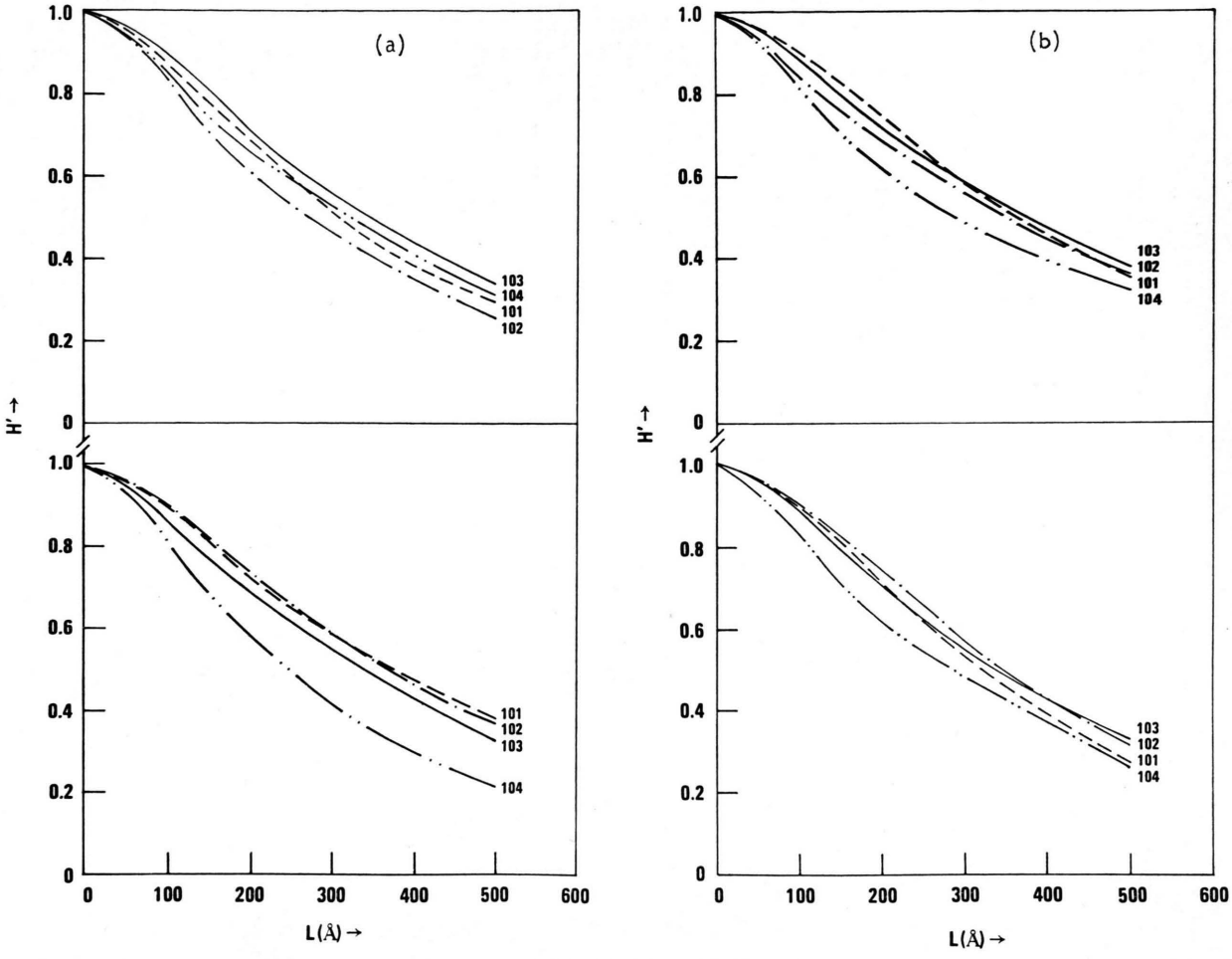

Fig. 2. The plots of total Fourier coefficients of Cd thin films. (a) Film A (top) and Film B (bottom); (b) Film C (top) and Film D (bottom).

The amount of anisotropy in $\bar{e}_L$ for the three directions included here is quite significant compared to that in D. We shall, therefore, retain the directional dependence of $\bar{e}_L$, but take the average value $\bar{D}$ for subsequent discussions. These data are displayed in Figure 3.

From the data we see that microstrains fall very rapidly with thickness in the initial stage. They, however, reach respective "saturation values,, above about 25,000 Å. The particle size, on the other hand, increases first becoming almost saturated at about the same value of thickness. These two effects together suggest that source of the structural disorder, which in this case is the thermally induced one, attains a stable equilibrium at this thickness. The microstrain decreases by about 50%, but the particle size increases only about 14% in this thickness range. This fact is the result of a two step process. In the first step, part of the disorder is released by rearrangement of the atoms towards the minimum potential energy during deposition of the films; in the second step the Cd atoms form some kind of coherently diffracting domains, whereby some atomic planes conveniently follow preferred orientation. This latter step presumably causes a change in the size of the various domain volume. What we have discussed above in terms of particle size is actually $\bar{D} = (V)^{1/3}$, where V is average volume of the domains, and it is measured in a direction perpendicular to the diffracting plane.

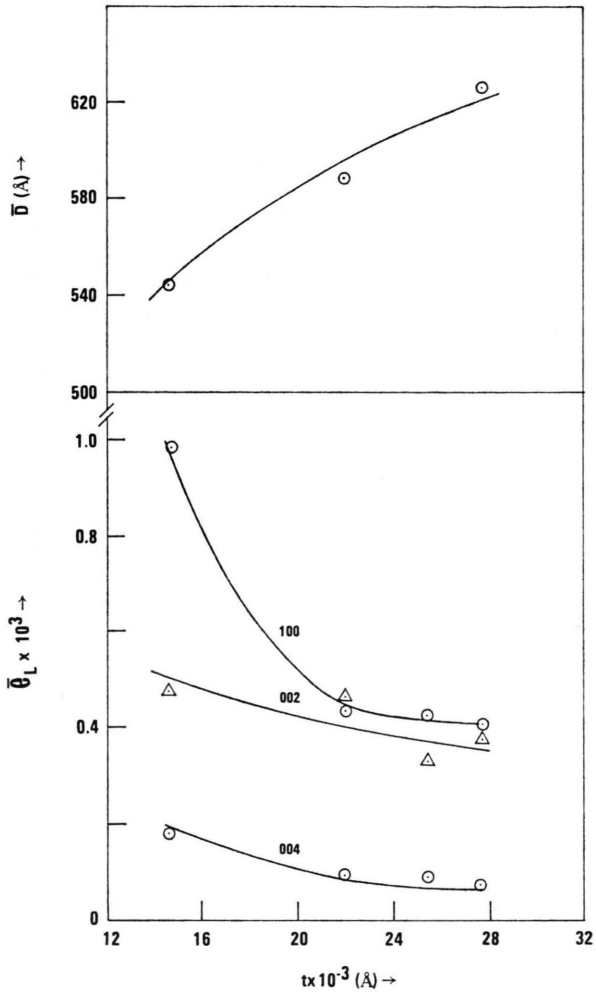

Fig. 3. Variation of average particle size $\bar{D}$ and microstrain $\bar{e}_L$ as function of film thickness. $\bar{D}$ was not found to have any directional dependence as $\bar{e}_L$.

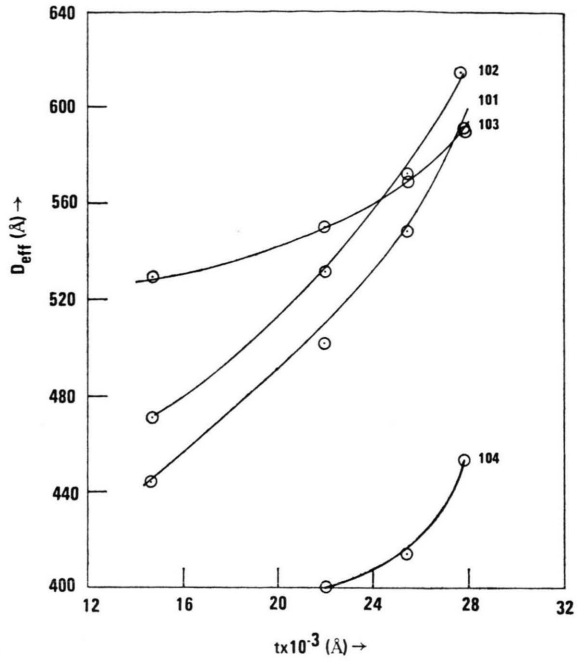

Fig. 4. Dependence of effective particle size D_{eff} on film thickness showing the influence of various crystal directions. D_{eff} refers to the reflections with faulting.

4.4. *Deformation and Growth Faults*

If we were to take Eq. (4.3) for 101, 102, 103 and 104 reflections it would directly give

$$(\partial H_r'(L)/\partial L)_{L=0} = (\partial H'(L)/\partial L)_{L=0} = -1/D_{eff} \qquad (4.6)$$

where

$$1/D_{eff} = 1/\bar{D} + 1/D_F . \qquad (4.7)$$

In Eq. (4.7) D_F is the fault size that includes the deformation fault probability α and growth fault probability β,

$$1/D_F = (|l|\, d_{hkl}/c^2)(3\alpha + \beta) \quad \text{for 101 and 103} \qquad (4.8a)$$

or

$$1/D_F = (|l|\, d_{hkl}/c^2)(3\alpha + 3\beta) \quad \text{for 102 and 104} . \qquad (4.8b)$$

Physically what α and β represent is this. Since in hcp structures, 002 planes form close packed layers with stacking sequence ABABABAB, a growth fault indicates a stacking disorder from AB to BC resulting in a new sequence ABABCBCB. Alternatively, another possibility exists, that is deformation fault, which forms the sequence ABABCACA instead of the other. The calculated values of $\bar{D}$ and D_F are shown in Table 5. As it has been accomplished earlier, the particle size $\bar{D}$ did not seem to contain strong directional dependence. We have, therefore, conveniently used this result to compute D_F, and hence α and β.

The plots of the fault parameters $(3\alpha+\beta)$ and $(3\alpha+3\beta)$ are shown in Figure 5. Once again, a strong directional dependence is observed, which is as significant as the microstrain calculation. Therefore, no attempt will be made here to suppress this in computing the individual probabilities α and β, which requires two sets of reflections in the same crystal direction. These fault parameters, however,

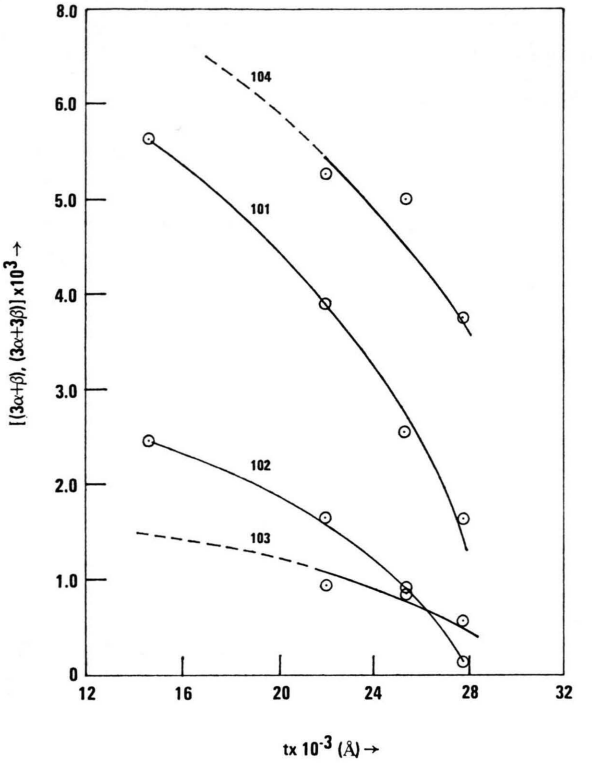

Fig. 5. The plots of fault parameters $(3\alpha + \beta)$ and $(3\alpha + 3\beta)$ as function of film thickness.

do indicate that both α and β diminish rapidly with thickness following

$$(3\alpha + \beta) \quad \text{or} \quad (3\alpha + 3\beta) = A - Bt - Ct^2 \tag{4.9}$$

relations, where t is the thickness and the constants $A \sim 10^{-3}$, $B \sim 10^{-8}$ Å^{-1} and $C = 10^{-12}$ Å^{-2}.Their exact values may be determined by actual curve fitting procedure. This interpretation is consistent with the earlier arguments proposed for microstrain and particle size. Apparently, both α and β have the same order of magnitude $\sim 10^{-3}$ and equal degree of effect on faulting.

4.5. Peak Shifts and Spacing Faults

One of the important quantities in the x-ray line broadening analysis is the peak shift. The plots of 2θ against thickness are found to be linear for all reflections over the entire thickness range. No noticeable change was observed for 002 and 004 reflections. The shift for 100 reflection is rather small compared to 101, 102, 103 and 104 reflections.

Theoretical works [26] on hcp structures suggest that for infinite crystal size, random fault distribution and extension of faults over the entire domain size, the lattice parameter c would be affected according to the relation

$$c = c_0(1 + \alpha' \delta') \tag{4.10}$$

where c_0 is the theoretical value in absence of disorder, α' is the layer fault probability and δ' is a theoretical constant less than unity. A layer fault consists [1, 2] of two parts: first a change in interplanar spacing called spacing fault, and secondly a change in the stacking sequence of atomic planes called stacking faults. We have already seen before that the stacking faults are described by deformation and growth faults. The peak shifts $\Delta(2\theta) = (2\theta)_{\text{theo}} - (2\theta)_{\text{obs}}$ are shown to be

$$\Delta(2\theta^0) = -\frac{720}{\pi}\left(\frac{l^2 d_{hkl}^2}{c^2}\right) \cdot (\tan\theta)\,\gamma'\,\delta' \quad \text{for} \quad h - k = 3N \tag{4.11a}$$

and

$$\Delta(2\theta^0) = \frac{360}{\pi}\left(\frac{l^2 d_{hkl}^2}{c^2}\right) \cdot (\tan\theta)\,\gamma'\,\delta' \quad \text{for} \quad h - k = 3N \pm 1 \tag{4.11b}$$

where N is an integer and

$$\gamma' = \alpha'(1 + \alpha') \approx \alpha' \quad \text{for} \quad \alpha' \ll 1\,. \tag{4.12}$$

Thus the above equations predict that, for $l = 0$, the shift $\Delta 2\theta = 0$, which should be satisfied by 100 reflection. Unfortunately, this does not appear to be the case. Furthermore, the theory [26] also predicts that reflections with $h - k = 3N$ should be shifted twice as much and in opposite direction as the reflections with $h - k = 3N \pm 1$. In the present study the data indicate that all shifts are unidirectional and positive, except 004. This departure is perhaps the consequence of inadequacy or inappropriateness of the spacing fault theory. We [1, 2] have arrived at a similar dilemma in our earlier study of polycrystalline Mg and Cd.

The peak shifts are vanishingly small for all reflections indicating a small probability for layer fault. The lattice spacings are observed to be linear function of thickness within the limits of our error bar and least square fit of the data. However, the unit cell ratio c/a remains constant at 1.8850 compared to its bulk value 1.8858. Witt and Vook [8] earlier suggested that peak shifts in thin films of hcp crystals could arise from thermally induced strains. Thus a small peak shift might be interpreted as due to small thermally induced strains.

5. Summary of the Results and Proposed Models

In the present investigation of vacuum deposited Cd thin films we have obtained several important results. First of all, the films of hcp metals are characterized by strong preferred orientation along the 002 planes parallel to the surface of the substrate, and that this preferred orientation is a strong function of thickness of the film. In particular, 100, 002, 004 peaks are many times stronger than their corresponding diffraction peaks obtained from polycrystalline powder samples. In face centered cubic (fcc) metals, however, 111 reflection shows the highest preferred orientation, and one can find what is known as "orientation factor" by determining the ratio of the integrated intensities between the most affected 111 reflection and the least affected 200 reflection. We have demonstrated in this work that the preferred orientation and geometrical broadening can be removed by deconvolution method using standard analytic forms of these functions. The effect of preferred orientation and geometrical broadening is shown to be coupled with the root mean square strain term. While a complete decoupling of each one of them is experimentally a formidable task, this difficulty nevertheless does pose no serious problem in working with Fourier analysis and investigating of other important effects, such as particle size, microstrain and faulting.

The thin films show a considerable x-ray line broadening due to thermally induced strain, which seemingly originates from a condition of mismatch of the thermal expansion between the glass substrate and Cd films. One way to represent this quantitatively would be two write [8] the thermal strain as

$$e_T = a_{ik}\, a_{jl}(\alpha_f - \alpha_g)\, \Delta T \tag{5.1}$$

where a_{rs} are rotation matrices which are defined by Witt and Vook [8]. Furthermore, α_f and α_g are respectively the linear thermal expansion of the film and glass, and ΔT is the difference in temperature, usually it is about $40 \sim 300\,°C$. We assume the average value of the thermal expansion coefficient for Cd bulk $\alpha_f = 30 \times 10^{-6}/°C$ and that for ordinary glass $\alpha_g = 9 \times 10^{-6}/°C$ and a probable range of temperature $\Delta T = 50\,°C$. Apparently, since we are considering the thermal expansion effect along the plane of the substrate, an additional factor of 4 should be introduced into Eq. (5.1) according to Witt and Vook [8]. In this way, we can estimate the microstrain in the films to be

$$e_T \sim 4 \times 10^{-3}\,. \tag{5.2}$$

Indeed, the order of magnitude of e_T is quite close to the present microstrain calculation.

To the knowledge of this author, no other detailed study on thin films of hcp metal is available. There are a few studies on thin films of some fcc metals, for example, Cu, Ag, Au and Al. We shall first compare our results with those of fcc metals and then propose interpretation of these results. Gangulee [11] has made a comparative study between electroplated and evaporated Cu film. He found for fcc Cu films a decrease of microstrain (which was actually the root mean square strain in his analysis) with film thickness. Furthermore, Cu films indicated no stacking faults, extrinsic- or intrinsic-type, although Cu bulk did show appreciable faulting in earlier studies [27, 28]. In Cd films we found a definite evidence of stacking faults, both α and β, in contrast to Cd bulk where only α has been detected [1]. For Ag, however, stacking faults have been detected in films [5] as well as in bulk [29, 30]. In this respect, Gangulee's interpretation that the strain anisotropy that promotes stacking faults in polycrystalline samples should collapse into undissociated dislocation loops, does not appear to hold. Alternatively, we find that the strain anisotropy in Cd film is much stronger than in Cd bulk, and consequently suggest that increase of anisotropy at the expense of unfavorable dislocation loops generates more of stacking faults. It should be remarked that for Cd bulk $\alpha \sim 3 \times 10^{-3}$ and $\beta \sim 0$.

The lattice parameters in Cd films increase with thickness. Light and Wagner [5], and Sen et al. [12] found that it decreases in Ag films with thickness. Walker [10] observed an increase in Al films with thickness. Vook and Witt [8] noted a decrease in Au films with thickness. From these results it will be sufficient to say that there is no a priori reason to believe that the lattice parameter would go either way with thickness. What can be said, at least, is this, that the behavior of lattice parameter is intrinsically related to the strain anisotropy and faulting of the films. It has been suggested by Walker [10] that in thin films the amount of scattering of the points representing various reflections on either side of the linear plot between lattice

parameter and Nelson-Riley function is a strong evidence of fault being present in the sample. We believe that it is the combination of the various weighting factors of the individual fault probabilities that should determine the negative or positive deviation of the lattice parameter from the bulk sample.

The particle size in Cd films is approximately of the same order of magnitude as in Cd bulk; but in Cu film the particle size was found [11] to be much smaller than that in Cu bulk. We postulate that the line broadening in Cd films is due predominantly to strain anisotropy and faulting, whereas in Cu films it is due primarily to particle size. This interpretation may be further substantiated by the fact that particle size in Cd films changes only by 14% against a substantial change of 50% of the microstrain for the thickness range incorporated in this study.

As mentioned above, for fcc metals the ratio

$$R = (\text{Intensity})_{111}/(\text{Intensity})_{200} \qquad (5.3)$$

has been used [11] as preferred orientation parameter, which decreased with film thickness for Cu films. Alternatively what we have proposed is a parameter S through Eqs. (3.15) and (3.19). It might be possible to get an idea as to the nature of variation of S with thickness if some way we can get an estimated value of K. Unfortunately, K is a very complicated geometrical parameter, whose only approximate form is described by Equation (3.24). We are, at present, working on this part of the problem with Cd and Mg films and hopefully will report our results in future publications.

In summary, we would like to reiterate that we have been able to study structural properties of Cd films with high degree of success by x-ray line broadening analysis. For the first time, we have shown that both the sine and cosine components of the Fourier coefficients are equally important, and that the effect of preferred orientation and geometrical broadening can be accounted for by Fourier coefficients of some appropriate analytic functions.

Acknowledgements

The author acknowledges his gratitude to two of his graduate students, S. H. Hunter who first did the preliminary part of the experiment, and M. Pita who helped at various stages of computations.

[1] N. C. Halder and S. H. Hunter, Z. Naturforsch. **29a**, 1771 (1974).
[2] N. C. Halder and E. E. Johnston, Z. Naturforsch. **30a**, 825 (1975).
[3] N. C. Halder and C. N. J. Wagner, Adv. X-ray Anal. **9**, 91 (1966); C. N. J. Wagner and E. N. Aqua, Adv. X-ray Anal. **7**, 46 (1963).
[4] C. N. J. Wagner, Local Atomic Arrangements Studied by X-ray diffraction, Eds. J. B. Cohen and J. E. Hilliard, Gordon and Broach, New York 1965.
[5] T. B. Light and C. N. J. Wagner, J. Vac. Sci. Tech. **3**, 1 (1965); J. Appl. Cryst. **1**, 199 (1968).
[6] P. Croce, G. Devant, M. Gandais, and A. Maraud, Acta Cryst. **15**, 424 (1962).
[7] P. J. Dobson and B. J. Hopkins, Brit. J. Appl. Phys. **1**, 1241 (1968).
[8] R. W. Vook and F. Witt, J. Vac. Sci. Tech. **2**, 49 (1965); J. Vac. Sci. Tech. **2**, 243 (1965); J. Appl. Phys. **39**, 2773 (1969); J. Appl. Phys. **40**, 709 (1969).
[9] N. W. Grimes, J. M. Pearson, R. W. Fane, and W. E. J. Neal, Phil. Mag. **21**, 178 (1970).
[10] G. A. Walker, J. Vac. Sci. Tech. **7**, 465 (1970).
[11] A. Gangulee, J. Appl. Cryst. **3**, 272 (1970); J. Appl. Phys. **43**, 867 (1972).
[12] S. Sen, S. K. Halder, and S. P. Sen Gupta, J. Phys. D: Appl. Phys. **6**, 1978 (1973).
[13] N. C. Halder, M. Pita and P. L. Li, Proc. Int. Conf. on Solid Films and Surfaces (Tokyo, Japan, 1978 to be published).
[14] A. K. Choudhuri and G. B. Mitra, Ind. J. Pure and Appl. Phys. **7**, 158 (1969).
[15] G. Marchetto, R. W. Vook, and R. Bourgault, J. Vac. Sci. Tech. **5**, 123 (1968); M. Atasagun and R. W. Vook, J. Vac. Sci. Tech. **7**, 362 (1970).
[16] H. P. Klug and L. E. Alexander, X-ray Diffraction Procedures for Polycrystalline and Amorphous Materials, John Wiley and Sons, New York 1974.
[17] B. E. Warren and B. L. Averbach, J. Appl. Phys. **21**, 595 (1950).
[18] R. Delhez, E. J. Mittemeijer, T. H. Keiser, and H. C. F. Rosenthal, J. Phys. E: Sci. Instrum. **10**, 784 (1977).
[19] R. Delhez and Mittemeijer, J. Appl. Cryst. **8**, 609 (1975); J. Appl. Cryst. **8**, 612 (1975); J. Appl. Cryst. **9**, 233 (1976).
[20] A. Guinier, X-ray Diffraction, W. H. Freeman Co., San Francisco 1963.
[21] B. E. Warren, X-ray Diffraction, Addison Wesley Pub. Co., Reading, Massachusetts 1969.
[22] T. H. de Keijser and E. J. Mittemeijer, Phil. Mag. **36**, 1261 (1977); Z. Naturforsch. **33a**, 316 (1978).
[23] R. Delhez and Mittemeijer, A Comparison of Two Methods for Separation of the $\alpha_1\alpha_2$ Dublet, private communication.
[24] B. Moraweck, P. de Montgolfier, and A. J. Renouprez, J. Appl. Cryst. **10**, 184 (1977).
[25] W. C. Sander, J. Appl. Phys. **37**, 1495 (1966).
[26] S. Lele, Acta Cryst. A **26**, 344 (1970).
[27] C. N. J. Wagner and J. C. Helion, J. Appl. Phys. **36**, 2830 (1963).
[28] C. N. J. Wagner, J. P. Boisseau, and E. N. Aqua, Trans. Met. Soc. AIME **233**, 1280 (1965).
[29] C. J. Newton and A. W. Ruff, Jr., J. Appl. Phys. **37**, 3860 (1966).
[30] C. N. J. Wagner, Acta Met. **5**, 477 (1957).